Sensors and Actuators B 145 (2010) 13–19

Contents lists available at ScienceDirect

Sensors and Actuators B: Chemical

journal homepage: www.elsevier.com/locate/snb

Gas sensing properties of thermally evaporated lamellar MoO_3

M.B. Rahmani[a,b], S.H. Keshmiri[b], J. Yu[a], A.Z. Sadek[c,*], L. Al-Mashat[a], A. Moafi[c], K. Latham[d], Y.X. Li[e], W. Wlodarski[a], K. Kalantar-zadeh[a]

[a] Sensor Technology Laboratory, RMIT University, Melbourne, Australia
[b] Microelectronics Research Laboratory, Physics Department, School of Sciences, Ferdowsi University of Mashhad, Mashhad, Iran
[c] Applied Physics, School of Applied Sciences, RMIT University, Melbourne, Australia
[d] Applied Chemistry, School of Applied Sciences, RMIT University, Melbourne, Australia
[e] Shanghai Institute of Technology, Chinese Academy of Sciences, Shanghai, China

ARTICLE INFO

Article history:
Received 16 June 2009
Received in revised form 3 November 2009
Accepted 4 November 2009
Available online 10 November 2009

Keywords:
Gas sensors
Molybdenum oxide
Thermal evaporation

ABSTRACT

In this work, MoO_3 was thermally evaporated onto gold interdigital fingers on quartz substrates and characterized using X-ray diffraction (XRD), scanning electron microscopy (SEM), and transmission electron microscopy (TEM) techniques. The deposited MoO_3 consist of stratified long rectangles (average length of 50 μm width of 5 μm and thickness of 500 nm) which are predominantly orthorhombic (α-MoO_3). Each of these plates was composed of many nano-thick layers (average ~30 nm) placed by Van der Waals forces on top of each other forming lamellar patterns. The devices were used as sensors and exhibited considerable change in surface conductivity when exposed to NO_2 and H_2 gases at elevated temperature of 225 °C. The structural and gas sensing properties of thermally evaporated MoO_3 thin films were investigated.

1. Introduction

Semiconductor metal oxide thin films have been extensively used for gas sensors as their conductivity changes due to interactions with gas molecules [1,2]. Such sensors also offer low cost, easy fabrication and consistent performance with respect to other type of gas sensors. Recently, there is an increasing trend to use specifically engineered structured materials as gas sensing elements [2–5]. The use of such structured materials such as belts, rods and wires in micro-, meso- or nano-dimensions, offer high surface to volume ratios and unique structural features that are expected to enhance the properties and performance of gas sensors [6–8]. Such structured oxide based chemical sensors were also found to decrease the device response time due to rapid diffusion of gaseous species into the materials' micro-, meso- and nano-porosities [5,6].

Among the semiconductor metal oxides, MoO_3 with a band gap energy of 2.39–2.9 eV is an excellent candidate for catalytic, electrochromic and gas sensing applications [9,10]. MoO_3 has been well known for its application as a catalyst for the oxidation of hydrocarbons and reduction of NO_x in the chemical and petroleum industry [11–14]. Efforts were also made to examine and improve the gas sensing properties of MoO_3 based devices to detect H_2 [10,15], CO [15,16], NH_3 [10,12,17], and LPG [10]. Imawan et al. [17] studied the RF sputtered MoO_3 thin films for sensing responses to various gases, including CO, CH_4, SO_2, NO_2 and NH_3 in the temperature range of 250 °C and 475 °C. They revealed that MoO_3 was highly sensitive to NH_3 at 425 °C and that the gas sensitivity dropped with decreasing film thickness (<300 nm). Multilayered sputter deposited MoO_3 by the same research group resulted in improved H_2 sensing properties and low cross sensitivity towards NH_3 [15]. It is also shown that the sensitivity and selectivity to target gases can be altered by adding other metal oxides to MoO_3 [1,18,19].

A number of techniques was reported for the deposition of MoO_3 including pulse laser deposition [12], thermal evaporation [20], sputtering [21], sol–gel [1,22], spray pyrolysis [23], chemical vapour deposition [24,25], and electro-deposition [26]. The deposition of MoO_3 using evaporative techniques is advantageous as it can produce highly crystalline and stratified structures. This is an important feature since high crystallinity and having layered formation can allow for greater sensitivity. MoO_3 can obtain an orthorhombic structure with double layers of linked MoO_6 octahedra (Fig. 1), parallel to [0 1 0] direction [10]. Each of these double layers consists of zig-zag chains along [0 0 1] of octahedra sharing edges. The double layers are held together by Van der Waals forces to make stratified structures [10,27].

The electrical conductance of a semiconducting oxide-based gas sensor depends on the chemisorbed oxygen ions, oxygen vacancies and the interstitial ions. The target gases change the oxygen balance of the oxide sensor, leading to a variation in its conductance. It is believed that in most of semiconducting oxide-based devices, the

* Corresponding author. Tel.: +61 3 99253690; fax: +61 3 99252007.
E-mail address: sadek@ieee.org (A.Z. Sadek).

0925-4005/$ – see front matter © 2009 Elsevier B.V. All rights reserved.
doi:10.1016/j.snb.2009.11.007

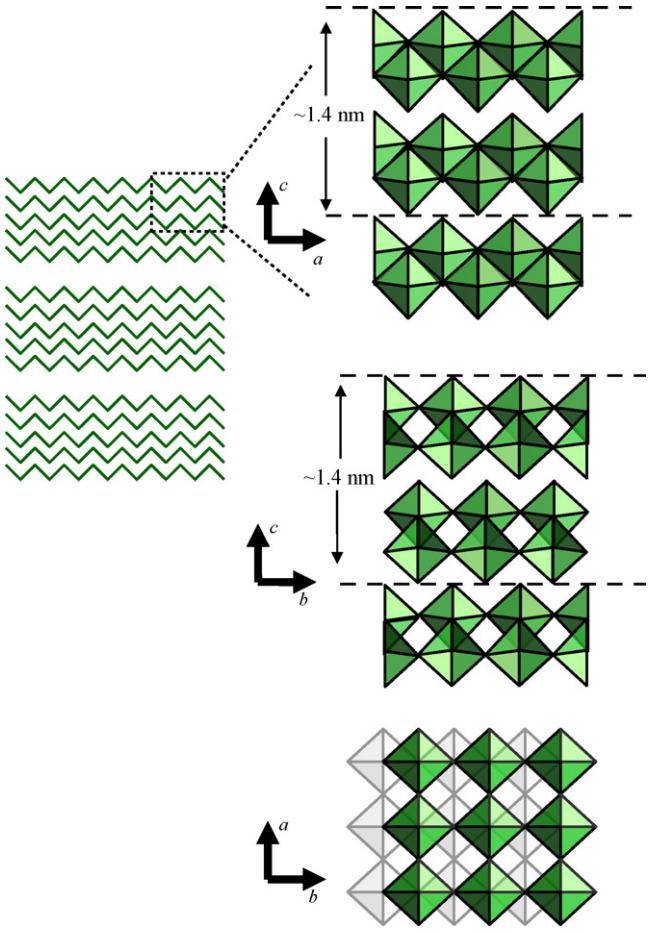

Fig. 1. Representations of α-MoO_3: the formation of secondary crystallite network (left) of edge- and corner-sharing MoO_6 octahedra viewed along different crystallographic planes (right). The secondary network (25 nm in our case) forms the tertiary thicker layers.

chemisorbed oxygen is involved in their sensing action at elevated temperatures [6,28,29].

In the case of a MoO_3 sensitive layer, direct adsorption has been proposed for oxidizing gases such as NO_2 and O_2 [7]. In such cases, oxidizing gases reduce oxygen defects [30]. Reducing gases such as H_2, typically react with adsorbed oxygen from the environment. Comini et al. [2] have studied gas sensing properties of MoO_3 nanorods deposited on alumina substrates toward CO and CH_3OH by varying the gas concentration between 10 and 1000 ppm at 40% relative humidity (RH) and at the working temperature of 200 °C. In the case of CO, they have utilized the common mechanism for oxide thin films to explain the gas sensing properties. According to this explanation, when CO is fed into the test chamber, the conductance of the MoO_3 layer increases, due to the exchange of electrons between the ionosorbed species and the semiconductor itself. CO reacts with oxygen species adsorbed on the semiconductor (O^{2-}, O^-, O_2^-) with a consequent increase in the conductance. However, a more accurate explanation has been presented by Choi and Thompson [31] who have studied changes in the MoO_3 surface using XPS in response to H_2. They observed that at 400 °C, the surface concentration of M^{6+} decreased and changed to lower oxidation states of Mo^{5+} and Mo^{4+}. This result indicates that the surface of MoO_3 is the most sensitive part of the crystal to be reduced by hydrogen. When oxygen is removed, orthorhombic MoO_3 is capable of forming shear structures, which facilitates the rearrangement of the polyhedra links: a change from corner-sharing octahedral either to edge-sharing or face-sharing octahedra. For MoO_6 octahedra, energy of the edge-linked system is considerably lower than the corner-linked system making the reaction highly favourable [10,32]. As a result, when MoO_3 is exposed to a reducing target gas, the involvement of its lattice oxygen can cause the change of conductivity. Reaction of MoO_3 at elevated temperatures has also been studied by different researchers [33,34] and it has been confirmed that in the range of 350–400 °C, the reaction on the surface of MoO_3 can lead to the appearance of surface domains forming crystallographic shear planes.

In this paper, the authors report about the response of MoO_3 thin films to low concentrations of NO_2 and H_2. It emerges that the film exhibit good response to these gases at the temperature range of 200–300 °C. In this work, thermal evaporation technique has been used for the deposition of MoO_3. Samples were characterized using X-ray diffraction (XRD), scanning electron microscopy (SEM), and transmission electron microscopy (TEM) techniques.

2. Experimental

Fresh quarts substrates were cleaned with acetone, isopropanol and DI water and consequently cut into 8 mm × 12 mm pieces for the deposition of MoO_3. An interdigital finger pattern of 100 nm thickness (gold/titanium) was deposited by sputtering and patterned by photolithography as the electrodes for conductometric sensing (Fig. 2).

MoO_3 powder (China Rare Metal Material Co.) was weighed at 10 mg and placed at the centre of a furnace at the temperature of 770 °C. The substrates were placed at a distance of 12 cm from the hot spot at a temperature of approximately 450 °C and thermal deposition was carried out using a carrier gas of 10% oxygen balanced in argon. Oxygen gas was added to the system to improve the stoichiometric formation of fully oxidized MoO_3. Deposition was carried out for a duration of 30 min and the evaporation temperature was increased slowly at the rate of 2 °C per min and cooled at the same rate after the procedure. A constant gas flow of approximately 800 sccm was utilized.

The SEM characterization was carried out using a FEI Nova NanoSEM. The TEM characterization was carried out using a JEOL JEM 1010 electron microscope. Samples for TEM were prepared by scratching the sample in ethanol, and subsequently drop casting the samples onto a Cu TEM grid. The XRD analysis was carried out using a Bruker D8 Discover microdiffractometer fitted with a GADDS (General Area Detector Diffraction System). Data was collected at room temperature using CuKα radiation (λ = 1.54178 Å) with a potential of 40 kV and a current of 40 mA, and filtered with a

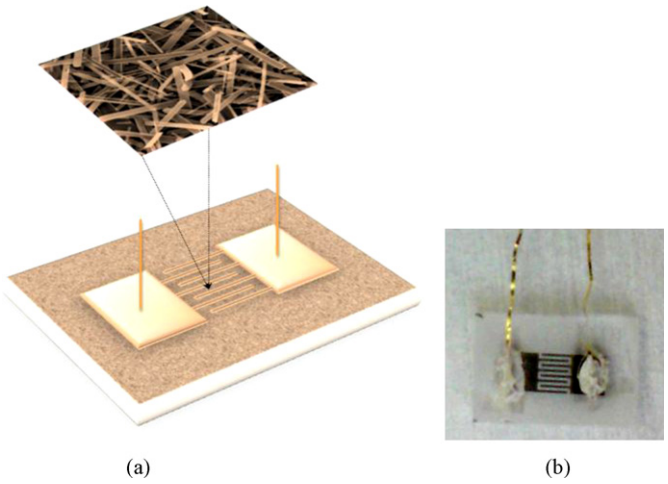

Fig. 2. (a) Schematic view and (b) picture of conductometric MoO_3 based sensor.

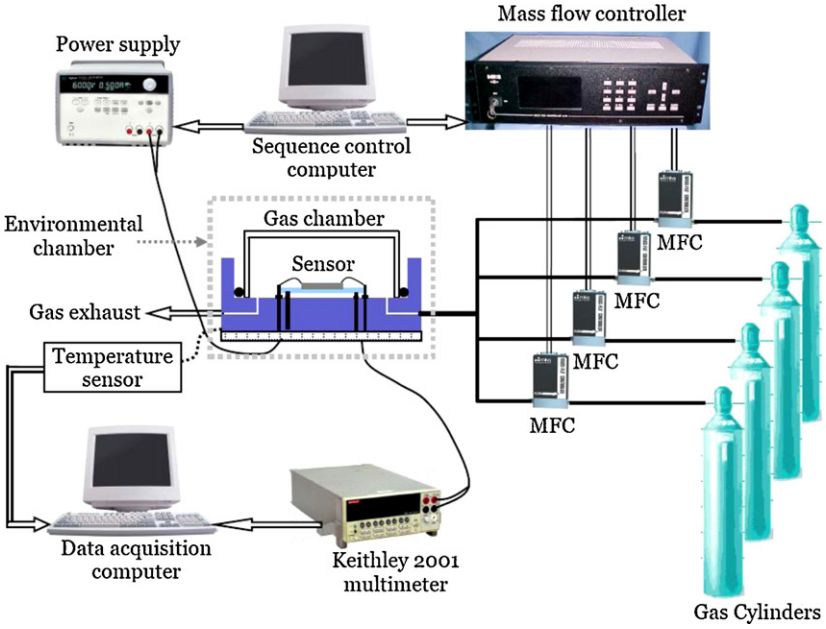

Fig. 3. Schematic view of multi-channel gas sensing measurement system.

graphite monochromator in the parallel mode (175 mm collimator with 0.5 mm pinholes).

MoO_3 conductometric sensors were mounted on an electric heater. Gas response measurements of the devices were performed in a test chamber made from Teflon, which was sealed in a quartz lid. The heater was controlled by a regulated DC power supply providing different operating temperatures. The output resistance as a function of time across the conductometric sensor during gas exposure was measured using a multimeter (Keithley 2001). A computerized gas calibration system, with mass flow controllers, was used for exposing the sensor to different concentrations of NO_2 and H_2 gases (Fig. 3). The total flow rate was kept constant at 200 sccm and dry synthetic air was used as the reference gas. At each operating temperature, the baseline gas was maintained for a duration of 120 min to allow the device to stabilize. Subsequently, the device was exposed to sequences of different concentrations of NO_2 and H_2 for several hours. The sensor temperature was varied in the 20–300 °C range. Each NO_2 gas sequence consisted of 0.6, 1.25, 2.5, 5 and 10 ppm balanced in synthetic air. A second pulse of 1.25 ppm was utilized to confirm its repeatability. Concentration of H_2 varied in the range of 0.06–1% balanced in synthetic air at constant gas flow of 200 sccm.

3. Results and discussion

3.1. Micro-characterization results

It is well known that gas sensing properties of a metal oxide thin film strongly depends on its morphological features. A high surface area facilitates the physisorption and chemisorption processes by increasing the absorption rates [1]. Fig. 4 shows the SEM morphological characterization on the as-deposited MoO_3 prepared by the thermal evaporation method. As can be seen, the MoO_3 thin film is composed of large rectangular plates with the average width and length of 5 and 50 μm, respectively. The inset in the Fig. 4(a) shows the typical thickness of the rectangles which is less than 1 μm (on average 500 nm for the previously described deposition condition), also it shows the layered nature of the rectangles. Fig. 4(b) clarifies that each of these plates were composed of many nano-thick layers with the average thickness of ~30 nm which form the main build-

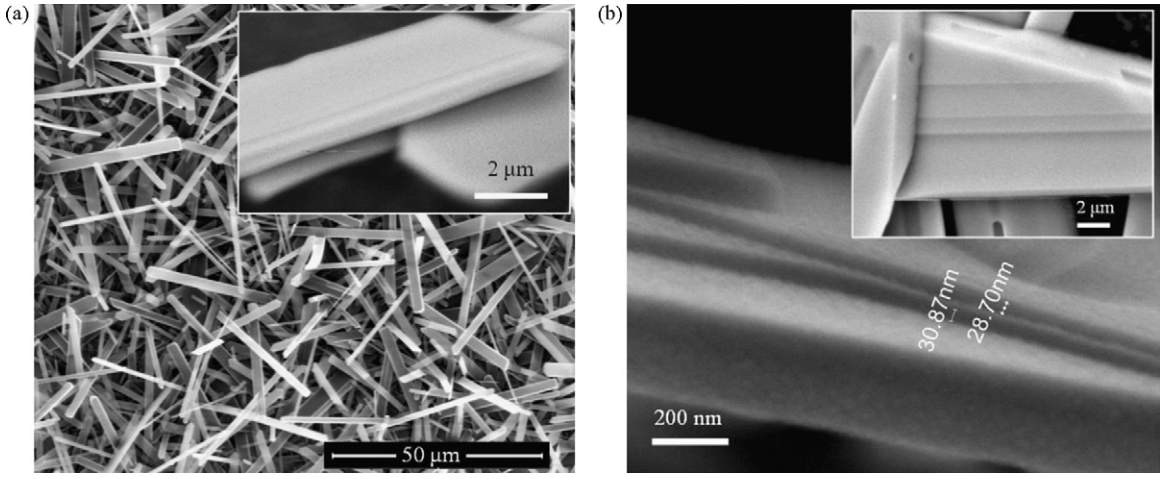

Fig. 4. (a and b) SEM micrographs of as-deposited MoO_3 structures, inset in (a) shows cross sectional SEM (45° rotation) of MO_3 thin film.

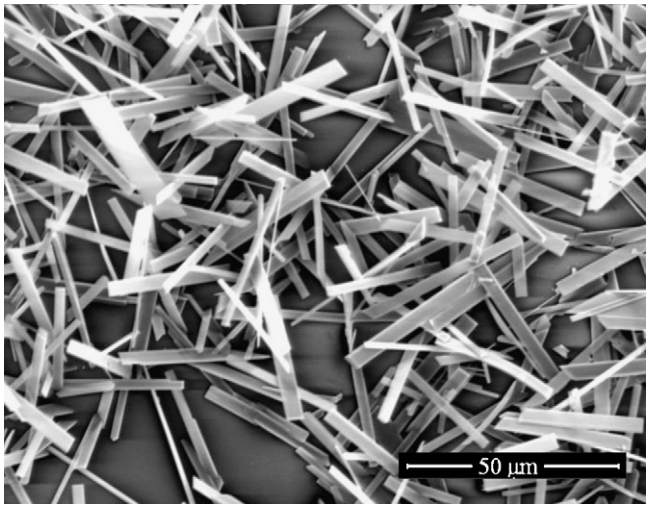

Fig. 5. SEM micrograph of MoO_3 sensor after a long term testing at 300 °C.

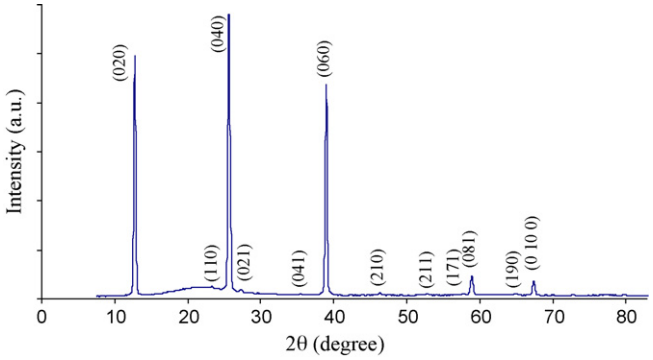

Fig. 6. XRD pattern of MoO_3 deposited by thermal evaporation.

ing blocks. It is suggested that such plates are placed by Van der Waals forces on top of each other forming lamellar patterns [10,27]. Mechanical exfoliation (similar to the exfoliation of graphene layers [35]) shows that our α-MoO_3 is made of secondary ~30 nm layers. Stacking of the fundamental double layers of α-MoO_3, which are 1.4 nm thick each (Fig. 1), forms these secondary layers. Thicker pieces (several hundreds of nm) are made of the secondary layers (SEM of an exfoliated layer is also shown in the SEM of the Siciliano et al.'s 2009 paper [36]).

Fig. 5 shows the surface of the MoO_3 sensor after a long term testing at temperatures as high as 300 °C. As can be observed the concentration of rectangles was decreased. The reason for the change can be attributed to the sublimation of MoO_3 from the sensor's surface due its low sublimation point. MoO_3 shows significant sublimations at temperatures above 700 °C [1].

Fig. 6 shows the XRD pattern of the MoO_3 deposited by thermal evaporation. The peaks were indexed to orthorhombic (α-MoO_3) crystal structure with lattice parameters of a = 3.962 Å, b = 13.858 Å, c = 3.697 Å (JCPDS Card No. 005-0508). The strong diffraction peaks of MoO_3 appear at 12.80, 25.70, 39.00, 58.90 and 67.40° 2θ, which correspond to the (0 2 0), (0 4 0), (0 6 0), (0 8 1) and (0 10 0) planes, respectively. This reveals that α-MoO_3 long rectangles grow with a strong preferred orientation. The respective peaks have been compared to literature indicating the existence of orthorhombic MoO_3 structures and an α phase. The strong intensity of the reflection peaks of (0 k 0) with k = 2, 4 and 6 proves the existence of the lamellar structure [37].

The average crystallite size of the film, which in this case is the thickness of the fundamental secondary layers, can be assessed using the Scherrer's formula [23,36]:

$$G_{h\ k\ l} = \frac{0.9\lambda}{\beta \cos\theta} \quad (1)$$

where $G_{h\,k\,l}$ is the average linear dimension of the crystal perpendicular to the diffracting plane ($h\,k\,l$), λ = 1.5406 Å is the wavelength of the X-ray radiation used and β is the angular full width of the diffraction peak at the half maximum (FWHM) for the diffraction angle 2θ. From the XRD spectrum, the assessed thickness of the fundamental secondary layers is approximately 25 nm. As a result, the secondary layers are made of the stacking of about 20–25 of the 1.4 nm fundamental double layers of α-MoO_3 (hence thickness of 25–30 nm). The tertiary large layers (up to several hundreds of nm) are formed from the stacking of these secondary layers. This is also confirmed by the SEM images. Such an observation was also reported by Siciliano et al. [36]. However, they suggested that their main building blocks had the thickness of 85 nm, possibly due to their different deposition conditions.

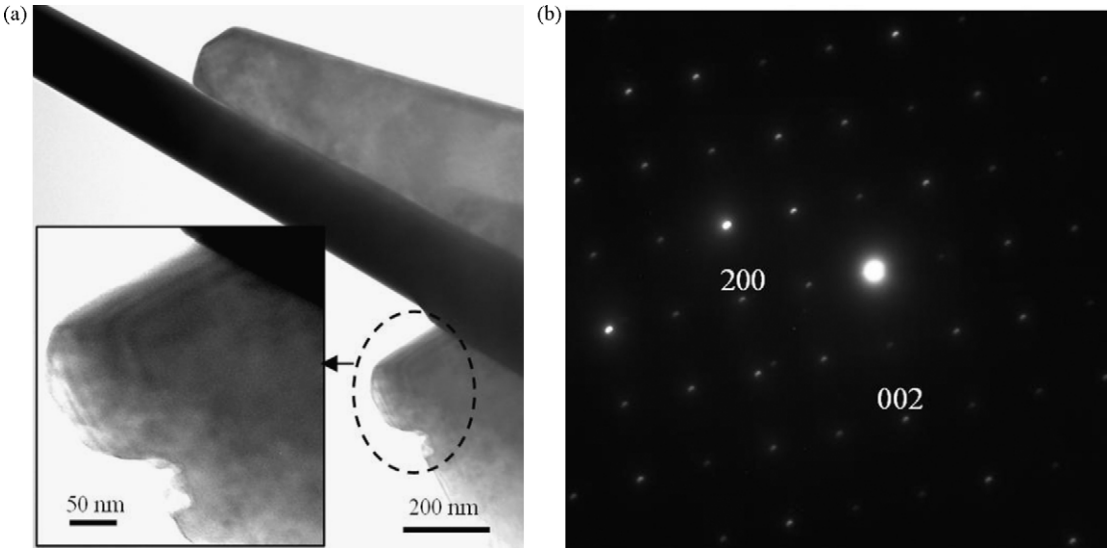

Fig. 7. (a) TEM image of MoO_3 long rectangles and (b) SAED pattern recorded from a thin area.

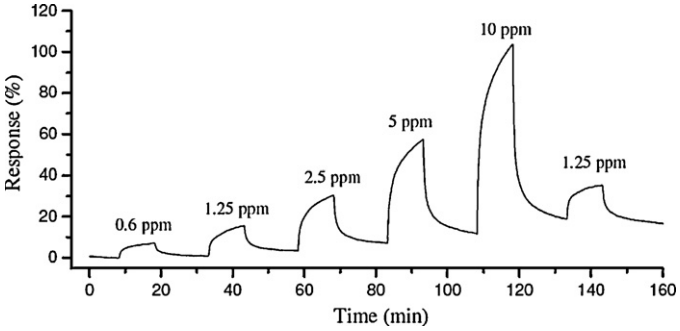

Fig. 8. Dynamic response of the MoO_3 sensor towards different concentrations of NO_2 gas at 225 °C.

Further characterization of the MoO_3 sensitive film was performed using TEM. A typical TEM image of the MoO_3 long rectangles is depicted in Fig. 7(a) with the corresponding surface area electron diffraction pattern (SAED) recorded on the thin area (Fig. 7b). The SAED pattern recorded perpendicular to the growth direction of the structure. It can be attributed to the [0 1 0] zone axis diffraction of orthorhombic MoO_3. Combined with the TEM information, the SAED study suggests that the long rectangles grow along the [0 0 1] direction, which is consistent with the XRD results [36,37].

3.2. Gas sensing results

The developed sensor was tested in a high temperature environment for a range between 180 and 300 °C. At the operating temperature below 180 °C, the resistance of the films was too high to measure (>1 GΩ). Additionally at very high temperatures (above 300 °C), the sensor's baseline was highly unstable and the resistance of the sample increased sharply which could be attributed to the sublimation of MoO_3 and deterioration of the long rectangles (Fig. 5). This observation has also been confirmed by other groups [1,29]. The optimum operating temperature for the sensor response towards H_2 and NO_2 was found to be 225 °C and the results are presented here. Figs. 8 and 9 show dynamic responses of the MoO_3 sensor towards different concentrations of NO_2 and H_2 at 225 °C, respectively. Upon the exposure to NO_2, the conductivity was decreased and when the sensor was exposed to H_2 gas it increased. The response factor of the sensor in percentage was defined as $S = (R_{gas} - R_{air}) \times 100/R_{air}$, where R_{gas} and R_{air} denote the resistance of the sensor in the presence of gas and air, respectively.

As discussed in the introduction, surface concentration of H_2 with MoO_3 surface transforms M^{6+} to lower oxidation states of Mo^{5+} and Mo^{4+}. In the temperature range between 100 and 500 °C oxygen chemisorbs over metal oxide, for example, in a molecular (O_2^-) and atomic form (O^-). Since O_2^- has a lower activation energy it is dominating at temperatures below 200 °C and at higher temperature the O^- form dominates [7]. In the MoO_3 sensor, change

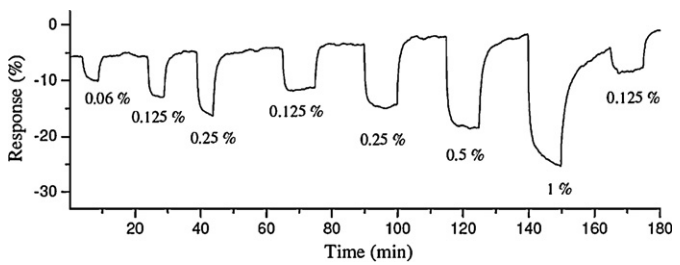

Fig. 9. Dynamic response of the MoO_3 sensor towards different concentrations of H_2 gas at 225 °C.

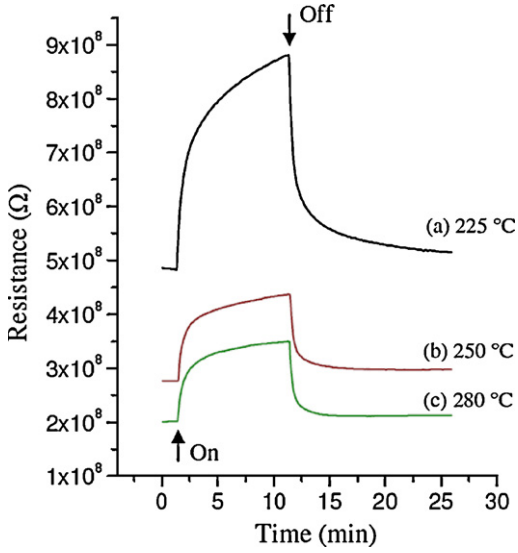

Fig. 10. Dynamic response of the MoO_3 sensor towards 10 ppm NO_2 gas at different temperatures.

in the oxygen balance of the oxide layer leads to a variation in its conductance. For H_2 gas the following interaction may take place:

$$H_{2(gas)} \rightarrow H_{2(ads)} \quad (2)$$

$$H_{2(ads)} + O^-_{(surface)} \rightarrow H_2O + e^- \quad (3)$$

where $H_{2(gas)}$, $H_{2(ads)}$ and $O^-_{(surface)}$ represent the H_2 in gas phase, chemisorbed H_2 and surface oxygen ions, respectively. This overall effect releases electrons on the surface and increases the sensor's conductance. In the case of an oxidizing gas (NO_2), reactions directly take place on the oxide surface. During the interaction process, molecules consume conduction electrons and subsequently increase the depletion region at the surface, and the resistivity of the sensor increases as presented below [3]:

$$NO_{2(gas)} \rightarrow NO_{2(ads)} \quad (4)$$

$$NO_{2(ads)} + e^- \rightarrow NO_2{}^-{}_{(ads)} \quad (5)$$

The MoO_3 thin films exhibited a high response to NO_2 and also a considerable response to H_2. Maximum response was measured to be 118% for 10 ppm NO_2 and 24% for 1% of H_2 at 225 °C. It was also found that the MoO_3 based sensor produce repeatable responses of the same magnitude for both of the gases. Fig. 10 shows the dynamic response characteristics of the MoO_3 sensor towards 10 ppm of NO_2 gas at three different temperatures. As can be seen with increasing the operating temperature the response and the recovery times of the sensor increased, but the response decreased. Therefore, the trade-off between different parameters is needed in choosing the optimum operating temperature. Considering the previously reported works [11,15], our thermally evaporated porous MoO_3 produces larger responses towards NO_2 in comparison with sputtered films.

In order to improve the sensing parameters such as sensitivity, response and recovery time, selectivity and stability, further work should be carried out. It is suggested that the application of different catalysts should also be investigated.

4. Conclusion

Thermally evaporated MoO_3 based conductometric gas sensors were developed and their responses towards NO_2 and H_2 were investigated. The MoO_3 thin films consisted of high aspect ratio long rectangles with average length of 50 μm, width of 5 μm

and thickness of 500 nm. Each long rectangle is composed of several nanobelts on top of each other producing a lamellar pattern. The XRD analysis revealed that the MoO_3 thin films are predominantly orthorhombic (α-MoO_3) crystal structure. The sensors were tested in a range of temperature between 180 and 300 °C and the study shows that the optimum operating temperature was 225 °C. Maximum response was measured to be 118% for 10 ppm NO_2 and 24% for 1% of H_2 at 225 °C. The results demonstrate that the developed sensors are worthy for further study and commercialization.

References

[1] K. Galatsis, Y.X. Li, W. Wlodarski, E. Comini, G. Sberveglieri, C. Cantalini, S. Santucci, M. Passacantando, Comparison of single and binary oxide MoO_3, TiO_2 and WO_3 sol–gel gas sensors, Sens. Actuators B 83 (1–3) (2002) 276–280.

[2] E. Comini, L. Yubao, Y. Brando, G. Sberveglieri, Gas sensing properties of MoO_3 nanorods to CO and CH_3OH, Chem. Phys. Lett. 407 (4–6) (2005) 368–371.

[3] A.Z. Sadek, S. Choopun, W. Wlodarski, S.J. Ippolito, K. Kalantar-zadeh, Characterization of ZnO nanobelt-based gas sensor for H_2, NO_2, and hydrocarbon sensing, IEEE Sens. J. 7 (5–6) (2007) 919–924.

[4] J.G. Partridge, M.R. Field, J.L. Peng, A.Z. Sadek, K. Kalantar-zadeh, J. Du Plessis, D.G. McCulloch, Nanostructured SnO_2 films prepared from evaporated Sn and their application as gas sensors, Nanotechnology 19 (12) (2008) 125504–125508.

[5] A.Z. Sadek, W. Wlodarski, Y.X. Li, W. Yu, X. Li, X. Yu, K. Kalantar-zadeh, A ZnO nanorod based layered ZnO/64° YX $LiNbO_3$ SAW hydrogen gas sensor, Thin Solid Films 515 (24) (2007) 8705–8708.

[6] E. Comini, G. Faglia, G. Sberveglieri, Z.W. Pan, Z.L. Wang, Stable and highly sensitive gas sensors based on semiconducting oxide nanobelts, Appl. Phys. Lett. 81 (10) (2002) 1869–1871.

[7] E. Comini, Metal oxide nano-crystals for gas sensing, Anal. Chim. Acta 568 (1–2) (2006) 28–40.

[8] A.A. Tomchenko, G.P. Harmer, B.T. Marquis, Detection of chemical warfare agents using nanostructured metal oxide sensors, Sens. Actuators B 108 (1–2) (2005) 41–55.

[9] A.K. Prasad, P.I. Gouma, MoO_3 and WO_3 based thin film conductimetric sensors for automotive applications, J. Mater. Sci. 38 (21) (2003) 4347–4352.

[10] S.S. Sunu, E. Prabhu, V. Jayaraman, K.I. Gnanasekar, T.K. Seshagiri, T. Gnanasekaran, Electrical conductivity and gas sensing properties of MoO_3, Sens. Actuators B 101 (1–2) (2004) 161–174.

[11] M. Ferroni, V. Guidi, G. Martinelli, M. Sacerdoti, P. Nelli, G. Sberveglieri, MoO_3-based sputtered thin films for fast NO_2 detection, Sens. Actuators B 48 (1–3) (1998) 285–288.

[12] S.S. Sunu, E. Prabhu, V. Jayaraman, K.I. Gnanasekar, T. Gnanasekaran, Gas sensing properties of PLD made MoO_3 films, Sens. Actuators B 94 (2) (2003) 189–196.

[13] D.B. Dadyburjor, S.S. Jewur, E. Ruckenstein, Selective oxidation of hydrocarbons on composite oxides, Catal. Rev. Sci. Eng. 19 (2) (1979) 293–350.

[14] M.A. Larrubia, G. Ramis, G. Busca, An FT-IR study of the adsorption of urea and ammonia over V_2O_5-MoO_3-TiO_2 SCR catalysts, Appl. Catal. B 27 (3) (2000) L145–L151.

[15] C. Imawan, H. Steffes, F. Solzbacher, E. Obermeier, A new preparation method for sputtered MoO_3 multilayers for the application in gas sensors, Sens. Actuators B: Chem. 78 (1–3) (2001) 119–125.

[16] M. Ferroni, V. Guidi, G. Martinelli, P. Nelli, M. Sacerdoti, G. Sberveglieri, Characterization of a molybdenum oxide sputtered thin film as a gas sensor, Thin Solid Films 307 (1–2) (1997) 148–151.

[17] C. Imawan, F. Solzbacher, H. Steffes, E. Obermeier, Gas-sensing characteristics of modified-MoO_3 thin films using Ti-overlayers for NH_3 gas sensors, Sens. Actuators B: Chem. 64 (1–3) (2000) 193–197.

[18] C. Imawan, H. Steffes, F. Solzbacher, E. Obermeier, Structural and gas-sensing properties of V_2O_5–MoO_3 thin films for H_2 detection, Sens. Actuators B: Chem. 77 (1–2) (2001) 346–351.

[19] K. Galatsis, Y. Li, W. Wlodarski, C. Cantalini, M. Passacantando, S. Santucci, MoO_3, WO_3 single and binary oxide prepared by sol–gel method for gas sensing applications, J. Sol–Gel Sci. Technol. 26 (1–3) (2003) 1097–1101.

[20] J. Zhou, S.Z. Deng, N.S. Xu, J. Chen, J.C. She, Synthesis and field-emission properties of aligned MoO_3 nanowires, Appl. Phys. Lett. 83 (13) (2003) 2653–2655.

[21] A.K. Prasad, P.I. Gouma, D.J. Kubinski, J.H. Visser, R.E. Soltis, P.J. Schmitz, Reactively sputtered MoO_3 films for ammonia sensing, Thin Solid Films 436 (1) (2003) 46–51.

[22] A.K. Prasad, D.J. Kubinski, P.I. Gouma, Comparison of sol–gel and ion beam deposited MoO_3 thin film gas sensors for selective ammonia detection, Sens. Actuators B: Chem. 93 (1–3) (2003) 25–30.

[23] A. Bouzidi, N. Benramdane, H. Tabet-Derranz, C. Mathieu, B. Khelifa, R. Desfeux, Effect of substrate temperature on the structural and optical properties of MoO_3 thin films prepared by spray pyrolysis technique, Mater. Sci. Eng. B 97 (1) (2003) 5–8.

[24] K.A. Gesheva, T. Ivanova, A low-temperature atmospheric pressure CVD process for growing thin films of MoO_3 and MoO_3–WO_3 for electrochromic device applications, Chem. Vap. Deposit. 12 (4) (2006) 231–238.

[25] S. Ashraf, C.S. Blackman, G. Hyett, I.P. Parkin, Aerosol assisted chemical vapour deposition of MoO_3 and MoO_2 thin films on glass from molybdenum polyoxometallate precursors; thermophoresis and gas phase nanoparticle formation, J. Mater. Chem. 16 (35) (2006) 3575–3582.

[26] R.S. Patil, M.D. Uplane, P.S. Patil, Structural and optical properties of electrodeposited molybdenum oxide thin films, Appl. Surf. Sci. 252 (23) (2006) 8050–8056.

[27] D. Dhawan, S. Bhargava, J. Tardio, W. Wlodarski, K. Kalantar-Zadeh, Gold coated nanostructured molybdenum oxide mercury vapour quartz crystal microbalance sensor, Sens. Lett. 6 (2008) 231–236.

[28] S.R. Morrison, Selectivity in semiconductor gas sensors, Sens. Actuators 12 (4) (1987) 425–440.

[29] S. Barazzouk, R.P. Tandon, S. Hotchandani, MoO_3-based sensor for NO, NO_2 and CH_4 detection, Sens. Actuators B: Chem. 119 (2) (2006) 691–694.

[30] P.I. Goumo, Nanostructured polymorphic oxides for advanced chemosensors, Rev. Adv. Mater. Sci. 5 (2003) 147–154.

[31] J.G. Choi, L.T. Thompson, XPS study of as-prepared and reduced molybdenum oxides, Appl. Surf. Sci. 93 (2) (1996) 143–149.

[32] J. Haber, M. Witko, Quantum-chemistry and catalysis in oxidation of hydrocarbons, Acc. Chem. Res. 14 (1) (1981) 1–7.

[33] L. Volpe, M. Boudart, Compounds of molybdenum and tungsten with high specific surface area: I. Nitrides, J. Solid State Chem. 59 (3) (1985) 332–347.

[34] L. Volpe, M. Boudart, Compounds of molybdenum and tungsten with high specific surface area: II. Carbides, J. Solid State Chem. 59 (3) (1985) 348–356.

[35] K.S. Novoselov, D. Jiang, F. Schedin, T.J. Booth, V.V. Khotkevich, S.V. Morozov, A.K. Geim, Two-dimensional atomic crystals, Proc. Natl. Acad. Sci. U.S.A. 102 (30) (2005) 10451–10453.

[36] T. Siciliano, A. Tepore, E. Filippo, G. Micocci, M. Tepore, Characteristics of molybdenum trioxide nanobelts prepared by thermal evaporation technique, Mater. Chem. Phys. 114 (2–3) (2009) 687–691.

[37] Q.P. Ding, H.B. Huang, J.H. Duan, J.F. Gong, S.G. Yang, X.N. Zhao, Y.W. Du, Molybdenum trioxide nanostructures prepared by thermal oxidization of molybdenum, J. Cryst. Growth 294 (2) (2006) 304–308.

Biographies

Mohammad B. Rahmani received BSc in physics from Shahid Bahonar University of Kerman, Iran (2000), and MSc in solid state physics from Ferdowsi University of Mashhad, Iran (2004). He is currently PhD candidate at the Physics Department, School of Sciences, Ferdowsi University. His research interests include transparent semiconducting oxides, nanotechnology, chemical sensors and solar cells. He also took part in a six-month joint collaboration at the School of Electrical and Computer Engineering, RMIT University, Melbourne, Australia (2009) where he worked on metal oxide semiconducting materials.

Sayyed Hossein Keshmiri is an associate professor at the Physics Department, School of Sciences, Ferdowsi University of Mashhad, Iran. He received his PhD at the Pennsylvania State University, USA (1981). His research interests include semiconductors, chemical sensors, MEMS and photonic crystals.

Jerry Yu graduated from RMIT University in 2007 where he received a double degree of Applied Science (Applied Physics) and Engineering (Electronic Engineering). He is currently pursuing his PhD in electronics and communication engineering at RMIT University in nanotechnological devices. His research interests include the fabrication and characterization of nano-devices and nano-sensors.

Abu Z. Sadek received the MEng degree in telecommunications engineering from the University of Melbourne, Australia, in 2002, and the PhD degree in electronics and communications engineering from the RMIT University, Melbourne, Australia, in 2008. He is currently a research fellow at the School of Applied Sciences (Applied Physics), RMIT University. His research interests include chemical sensors, solar cells, nanotechnology, carbon nanotubes and conducting polymers.

Laith Al-Mashat received his BSc in electronics and communications engineering from University of Technology, Baghdad, Iraq in 1995. Since graduation he worked as an R&D engineer in several engineering firms. He is a professional engineer member of IEEE and the Institution of Engineers, Australia. He is currently a PhD candidate at RMIT University working on conducting polymer nanostructures for sensing applications.

Ali Moafi received his Masters in solid state physics in 2002. He is a PhD student in physics department at RMIT University, Melbourne, Australia. His field of research is the fabrication of high speed high performance materials and devices based on graphene. His other research interests include hydrogen sensors and thermal management in nano-systems.

Kay Latham received a PhD from the University of Wolverhampton in 1996, and a PGCE from Sidney Sussex College, University of Cambridge, in 1996. She is a charted chemist and member of both the Royal Society of Chemistry and the Royal Australian Chemical Institute. Kay is currently senior lecturer in the School of Applied Sciences (Applied Chemistry) at RMIT University. Her research interests involve many aspects of inorganic and materials chemistry, with a strong emphasis on synthetic methodology and structural characterization. At present the prime focus of

her work concerns metal oxide and phosphonate networks for application in sensor development.

Yongxiang Li received his PhD degree in electronics engineering from Xi'an Jiaotong University in 1991. He has carried out research in Germany and Australia, and is currently a professor at Shanghai Institute of Ceramics, Shanghai, China. His research interests currently focus on electronic materials and devices.

Wojtek Wlodarski has worked in the areas of sensor technology and instrumentation for over 30 years. He has published 4 books and monographs, over 400 papers and holds 29 patents. He is a professor at RMIT University, Melbourne, Australia, and heads the Sensor Technology Laboratory at the School of Electrical and Computer Engineering.

Kourosh Kalantar-zadeh is an associate professor at the School of Electrical and Computer Engineering, RMIT University, Australia. He received his BSc (1993) and MSc (1997) from Sharif University of Technology, Iran, and Tehran University, Iran, respectively, and completed his PhD at RMIT University, Australia (2001). His research interests include chemical and biochemical sensors, nanotechnology, microsystems, materials science, electronic circuits and microfluidics.